

Chemically Functionalized Clay Vinyl Ester Nanocomposites: Effect of Processing Parameters

D. YEBASSA,¹ S. BALAKRISHNAN,¹ E. FERESENBET,¹ D. RAGHAVAN,¹ P. R. START,² S. D. HUDSON²

¹Polymer Group, Department of Chemistry, Howard University, 525 College Street NW, Room 120, Washington, DC, 20059

²Polymers Division, National Institute of Standards and Technology, Gaithersburg, Maryland 20899

Received 27 May 2003; accepted 30 October 2003

ABSTRACT: The primary objective of this study was to improve montmorillonite clay-platelet separation in vinyl ester resin matrix by organically modifying the nanoclay platelet with a partially reactive onium salt. The reactive onium salt (ω -undecylenyl amine hydrochloride) was synthesized from commercial ω -undecylenyl alcohol through a series of synthetic conversions. Nonreactive onium salt (undecyl amine hydrochloride) was made from commercial undecyl amine. These salts were characterized with ¹H and ¹³C NMR and Fourier transform infrared techniques. The relative amounts of exfoliated, intercalated, and as-treated clay and the size of the clay particle aggregates depended significantly on the composition of clay and the processing conditions. When the clay was ion-exchanged with a mixture of reactive and nonreactive onium salts, a partially exfoliated vinyl ester resin polymer nanocomposite was formulated. The addition of a comonomer styrene and high-intensity ultrasonic mixing produced vinyl ester nanocomposite with the highest degree of clay-platelet exfoliation. © 2004 Wiley Periodicals, Inc. *J Polym Sci Part A: Polym Chem* 42: 1310–1321, 2004

Keywords: vinyl ester; nanocomposites; montmorillonite clay; WAXS; TEM

INTRODUCTION

Polymer nanocomposites are a relatively new class of materials obtained by dispersing a wide range of diverse nanoelements, for example, inorganic-layered silicates and organic carbon nanotubes, into polymeric resin.^{1,2} Often reported in the literature are the vast improvements in the properties of nano-element-filled polymers as compared with those of conventional filler-based polymer composites, for only a small mass-fraction percentage of nanoelement.^{3–7}

With clay as the nanoelement, organic–inorganic hybrid nanocomposites have been formu-

lated with various thermoplastic and thermoset polymers.^{3–20} The clay particles are essentially bundles of nanoclay sheets that are roughly 1 nm in thickness and 100–1000 nm in breadth. For example, an 8- μ m clay particle has approximately 3000 nanoclay sheets of 1 nm thickness and 20–200 nm in diameter.²¹ Because these hydrophilic clay sheets are not compatible with hydrophobic organic matrices, and the spacing between the clay sheets is extremely narrow, diffusion of polymer chains in the clay galleries is not likely. This often leads to aggregation of clay particles, and the aggregated clay sheets act as stress-concentration sites in the polymer matrix. When the clay sheets exist in such bundles and the original interlayer spacing of clay sheets is unaltered in polymer matrix, the composite is referred to as a *tactoid nanocomposite structure*. If the interlayer

Correspondence to: D. Raghavan (E-mail: draghavan@howard.edu)

Journal of Polymer Science: Part A: Polymer Chemistry, Vol. 42, 1310–1321 (2004)
© 2004 Wiley Periodicals, Inc.

spacing of clay sheets is increased and the clay sheets are poorly dispersed, the composite is referred to as an *intercalated nanocomposite*. If the clay sheets are well dispersed and distributed, the composite is referred to as an *exfoliated nanocomposite*. Generally, an exfoliated morphology of clay platelets is sought, with the expectation that this would improve nanocomposite properties.²² Therefore, the objective of this study was to improve clay-platelet separation by making the clay sheets compatible with vinyl ester resin.

Compatibility between the clay and polymer is achieved by an ion-exchange reaction of Na^+ , Ca^{+2} , or K^+ with a long-chain cation to increase the organophilicity of the clay-surface layer and provide sufficient layer separation for polymer chains to infiltrate. Until now, most of intercalation/exfoliation studies on nanocomposites have been carried out by exchanging the cations on clay with nonbonding ammonium salts. As expected, the clay gallery spacing increased as the grafted chain length of the ammonium salt on clay surface was increased.

Another approach commonly used in achieving clay-platelet separation is to suspend the clay particles in a polar solvent/monomer medium to promote the swollen polymer or the polymer formed during *in situ* polymerization to penetrate the clay galleries.²⁰ The criteria for solvent/monomer selection are based on its miscibility with the polymer and its ability to swell the organically modified clay.

Both these approaches are attractive, and they provide a framework to explore the role of the reactive onium salt in clay-platelet separation for vinyl ester nanocomposites. Very few studies have dealt with the role of a reactive onium salt that has a structural similarity or reactivity with the polymer resin in formulating polymer nanocomposites.⁴ The initial work by Toyota researchers in formulating nylon nanocomposites was based on the functionalization of montmorillonite clay with 12-aminolauric acid. This work clearly demonstrated the desirability of onium salts having a terminal functional group for clay-platelet separation. Although the role of reactive salts in nanocomposites can be inferred from this work, specific examples related to montmorillonite clay functionalized with vinyl-terminated ammonium salts for vinyl ester systems are not available in the open literature. In general, there have been few studies reported for vinyl ester nanocomposites.^{23,24} The concept of chemically coupling the functionalized clay sheet with the polymer or

polymer precursor can be useful in promoting the stress transfer to the reinforcement phase to improve the mechanical properties of the nanocomposite.

In this research, emphasis was placed on the synthesis of the surfactant and the role of the reactive, surfactant-modified clay over the nonreactive, surfactant-modified clay in promoting clay-platelet separation in clay vinyl ester nanocomposites. The nonreactive surfactant used was undecyl (C11) amine hydrochloride, whereas the reactive surfactant used was ω -undecylenyl (C11 with terminal vinyl) amine hydrochloride. The latter compound was synthesized from ω -undecylenol by a series of reactions that included bromination, azide formation, and azide reduction. A similar strategy has been used for the synthesis of amines from alcohols.^{25–27} Here, we report the synthesis and characterization of the intermediates and the surfactant molecule with an olefinic group at the terminal end from ω -undecylenol. The olefinic functional group in the reactive surfactant was expected to promote chemical coupling of the clay to the polymer matrix and thus better dispersion of the clay platelets in the polymer matrix. Efforts are underway to establish evidence for chemical coupling between functionalized clay and matrix resin and the findings of which will be presented in a later publication.

MATERIALS AND METHOD²⁸

Reagents

The ω -undecylenol was procured from Aldrich Chemical Co.²⁸ Lithium aluminum hydride, hexane, sodium azide, *N*-bromo succinimide, triphenyl phosphine, and diethyl ether were purchased from Fisher Scientific International. Some of the chemicals used for the study were high-purity grade.

Instrumentation

A Fourier transform infrared (FTIR) spectrophotometer (Nicolet-Magna IR 560 spectrometer from Thermo Nicolet Instrument Corp., Madison, WI) was used to obtain IR spectra. Liquid samples were run neat (NaCl plate), and solid samples were run with the KBr pellet method. Synthetic conversions were monitored with a Hewlett-Packard 5890 series II gas chromatograph (GC) coupled to a Hewlett-Packard 5989A mass

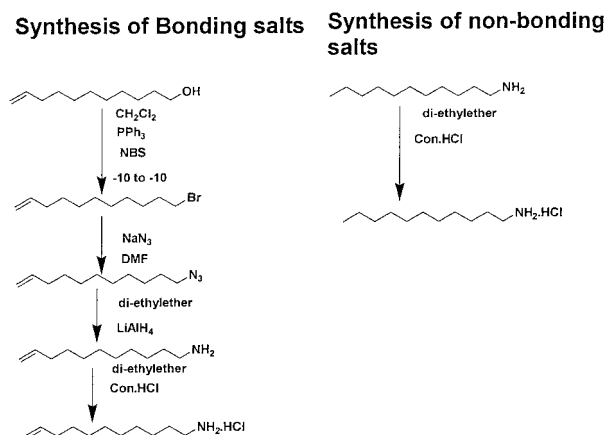


Figure 1. Reaction scheme for synthesizing undecylenyl amine hydrochloride and undecyl amine hydrochloride.

spectrometer (Avondale, PA). The interface oven and transfer line were set at 285 °C; the injection port set temperature was at 150 °C, in the electron-impact mode, with electron energy at 70 eV. High-resolution, capillary GC was conducted with a Supelco fused-silica SPB-1 (30 m, 0.32 mm i.d., 0.25- μ m film thickness) (Bellefonte, PA) as the column. The oven temperature was programmed 40 °C for 3 min, 20 °C/min to 300, and 300 °C for 1 min; the injector temperature was set at 240 °C, the detector temperature was set at 285 °C, and helium was used as the carrier gas with a head pressure of 69 kPa. By dissolving an aliquot of sample in dichloromethane and injecting 1 μ L of sample at the port, gas chromatography-mass spectrometry measurements were performed. ^1H and ^{13}C nuclear magnetic resonance (NMR) data were obtained with a General Electric 300-MHz NMR spectrometer (GE NMR Instruments, Fremont, CA). Deuterated chloroform was used as a solvent and source of internal reference in performing the NMR experiments for all the samples.

Synthesis of Undecylenyl Amine Hydrochloride

Figure 1 provides the reaction sequences used in the synthesis of ω -undecylenyl amine hydrochloride (reactive surfactant) from ω -undecylenol and undecyl amine hydrochloride (nonreactive surfactant) from undecyl amine.

Conversion of Undecylenyl Alcohol into Undecylenyl Bromide

The ω -undecylenyl alcohol was procured from Aldrich Chemical. In a dry, three-necked, 500-mL,

round-bottom flask equipped with a magnetic stirring bar and a nitrogen inlet, undecylenyl alcohol (9.164 g, 59 mmol) was dissolved in 120 mL of methylene chloride. Triphenyl phosphene (15.54 g, 65 mmol) was gradually added to the stirred mixture from -5 to -10 °C, while cooling the flask in an ice-salt jacket. Then, *N*-bromo succinimide (NBS) (10.19 g, 63 mmol) was gradually added to the mixture in the flask over a duration of 30 min while maintaining the temperature of the mixture below -5 °C by cooling the flask with the ice-salt mixture. Once NBS addition was complete, the resulting solution was allowed to warm to room temperature, after which stirring was continued for an additional hour. Methylene chloride was distilled until a white precipitate started to appear. Then, petroleum ether was added gradually to the mixture, and distillation continued until complete removal of methylene chloride was achieved. The mixture was filtered, and the white precipitate was washed with petroleum ether and collected with the filtrate. The filtrate was distilled to obtain liquid undecylenyl bromide. This bromide compound was then purified with a silica gel column with the aid of petroleum ether as a solvent and was assisted by purging with nitrogen gas on the top of the column. The purified bromide compound was used in the subsequent reactions; the yield was $88 \pm 3\%$.

^1H NMR of product: δ 1.1–1.4 (m, 12H), 1.8 (m, 2H), 1.9 (m, 2H), 3.3 (t, $J = 7$ Hz, 2H), 4.8 (m, 2H), 5.7 (m, 1H). IR (NaCl) (cm^{-1}): 3073, 3001, 2925, 2853, 1630, 1455, 1434, 1240, 989, 907, 743, 718, 646 [refer to Fig. 2(a,b)]. MS mass-to-charge ratio (m/z): 233 (M^+), 232 ($\text{M}-1$), 204, 190, 176, 162, 148, 135, 123, 111, 97, 83, 69, 55.

Conversion of Undecylenyl Bromide to Undecylenyl Azide

To a 500-mL, round-bottom flask equipped with a stirring bar, sodium azide (3.05 g, 47 mmol) and 230 mL of dimethylformamide (DMF) were transferred. To the stirred solution, undecylenyl bromide (7.3 g, 31.3 mmol) was added drop by drop, and the entire mixture was allowed to stir for 12 h. The azide mixture was then transferred to a 500-mL separatory funnel. The solution was extracted with ether and water at a 1:1 ratio in a separatory funnel. The ether layer was washed with water three times to remove DMF. The ether layer was collected and dried over anhydrous MgSO_4 and then distilled to obtain undecylenyl

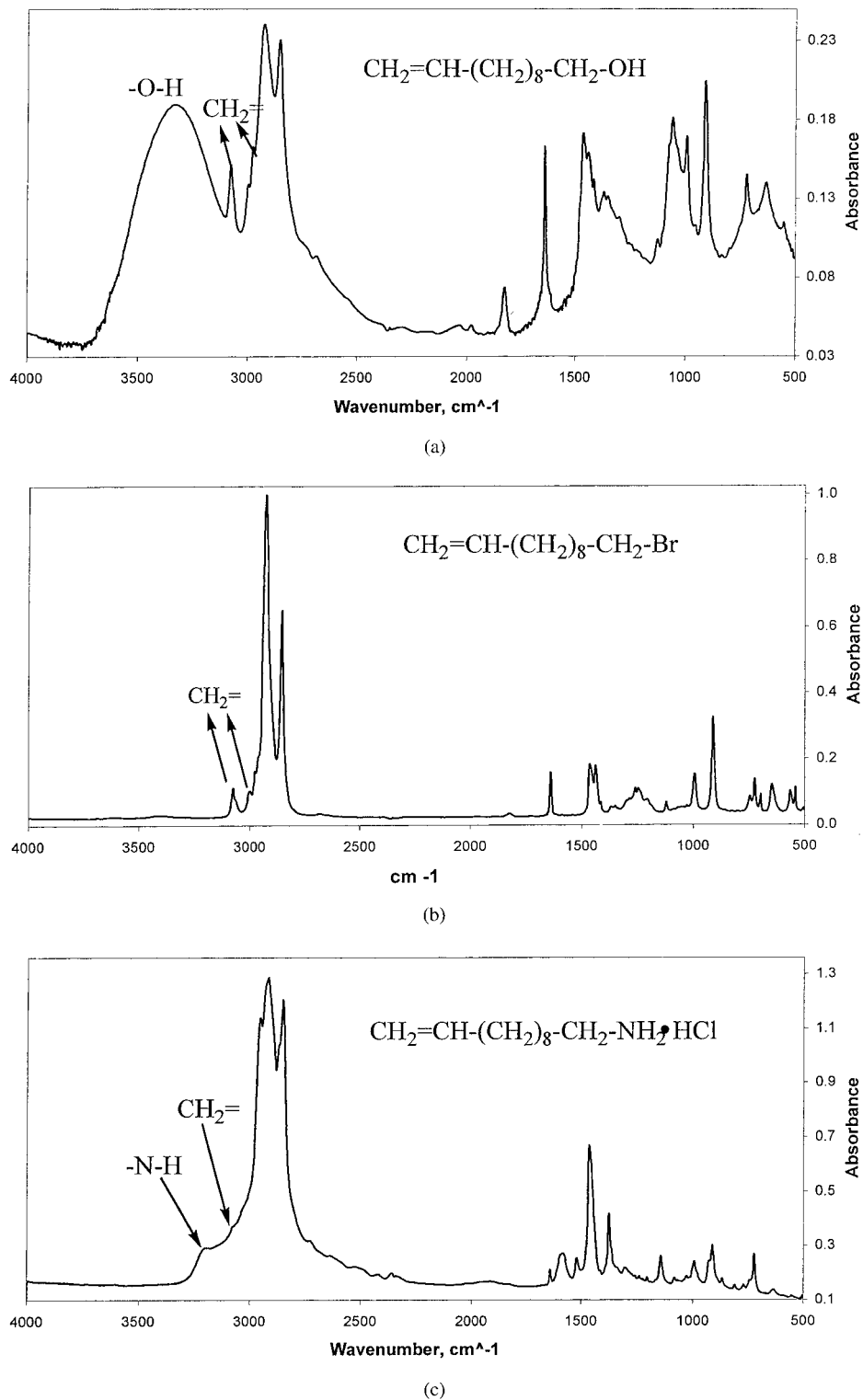


Figure 2. FTIR spectra of (a) undecylenyl alcohol, (b) undecylenyl bromide, and (c) undecylenyl amine hydrochloride.

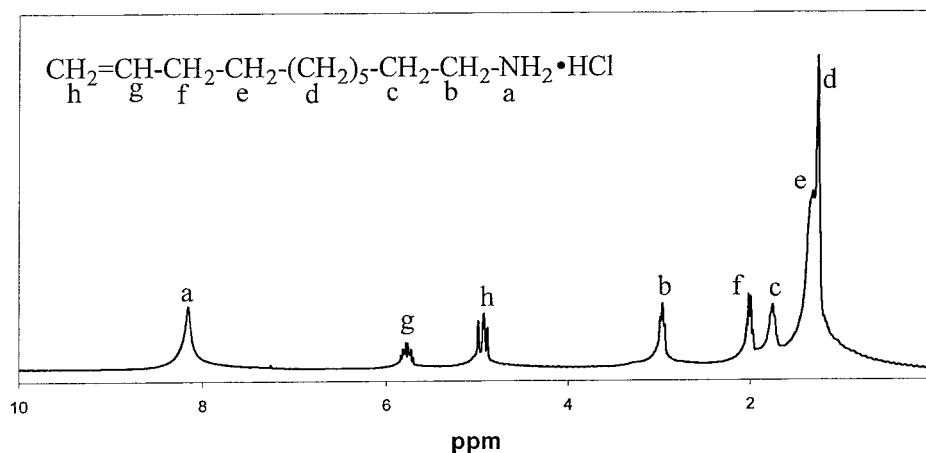


Figure 3. ^1H NMR spectrum of undecylenyl amine hydrochloride.

azide compound. The reaction was repeated several times, and the yield was $80 \pm 4\%$.

^1H NMR of product: δ 1.1–1.4 (m, 12H), 1.55 (m, 2H), 2.0 (m, 2H), 3.2 (t, $J = 7$ Hz, 2H), 4.9 (m, 2H), 5.8 (m, 1H). IR (NaCl) (cm^{-1}): 3083, 2935, 2853, 2095, 1644, 1465, 1347, 1260, 988, 902, 723, 636, 554. MS m/z : 194 (M-1), 168, 167, 166, 152, 138, 124, 110, 96, 84, 70, 55.

Conversion of Undecylenyl Azide to Undecylenyl Amine Hydrochloride

Lithium aluminum hydride (3.56 g, 64 mmol) was transferred to a two-necked, 500-mL flask, and 240 mL of ether were added. The reaction mixture was allowed to stir for 2 h. Then, undecylenyl azide (4.64 g, 24 mmol) was gradually added to the mixture and allowed to stir overnight. The

reaction mixture was quenched with drop-by-drop addition of 10 mL of water. This mixture was then allowed to stir for an additional 15 min. The organic layer was filtered, and an equivalent amount of concentrated HCl acid (24 mmol) was added. The organic layer was distilled to obtain ω -undecylenyl amine hydrochloride salt. The reaction was repeated several times, and the yield was $91 \pm 3\%$. The final compound was characterized with NMR and FTIR spectroscopies.

^1H NMR of product: δ 1.1–1.4 (m, 12H), 1.75 (m, 2H), 2.0 (m, 2H), 3.0 (t, $J = 7$ Hz, 2H), 4.9 (m, 2H), 5.8 (m, 1H), 8.2 (s, 3H). ^{13}C NMR (δ): 25.74, 28.77 (5C), 32.6, 33.5, 62.8, 114.0, 139.0 (see Figs. 3 and 4). IR (KBr pellet) (cm^{-1}): 3211, 2956, 2925, 2853, 1588, 1460, 1368, 1137, 994, 897, 712 [see Fig. 2(c)].

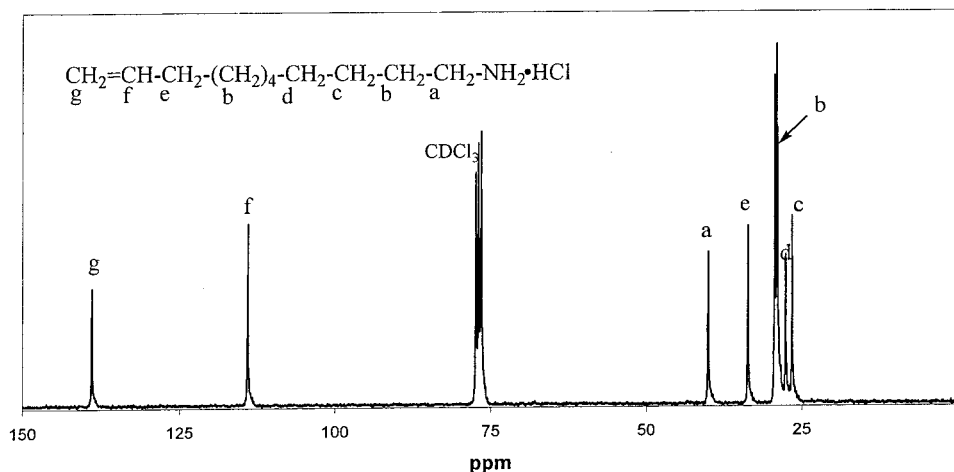


Figure 4. ^{13}C NMR spectrum of undecylenyl amine hydrochloride.

Synthesis of Undecyl Amine Hydrochloride

The undecyl amine (procured from Aldrich Chemical) was used without further purification to form undecyl amine hydrochloride with concentrated HCl. The undecyl amine hydrochloride was characterized by FTIR and ^1H NMR techniques.

^1H NMR of product: δ 0.9 (t, 3H), 1.24 (m, 16H), 1.78 (m, 2H), 3.0 (m, 2H), 8.2 (s, 3H). IR (KBr pellet) (cm^{-1}): 3211, 2920, 2904, 2853, 1598, 1501, 1460, 1050, 989, 912.

Preparation of C11 Clay

Na-montmorillonite (Na^+ -MMT) was provided by Southern Clay Products under the trade name of Sodium Cloisite (Na-Cloisite). Na-Cloisite has a cation-exchange capacity (CEC) value of 92 mmol/100 g of clay with the exchangeable sites ionically bound with Na cations.²¹

Na^+ -MMT is a fine powder with an average particle size of 13 μm . The preparation of partially reactive and nonreactive clay was performed by the ion exchange of Na^+ with the synthesized surfactant cations. To synthesize partially reactive C11 clay, Na^+ clay (7.5 g) was dispersed into 600 mL of distilled water at 80 ± 2 °C. ω -Undecylenyl amine hydrochloride (0.1565 g, 25 mol %) and undecyl amine hydrochloride (0.4518 g, 75 mol %) (referred to as partially reactive C11 clay, RC11) in 300 mL of distilled water maintained at 80 ± 2 °C was poured into the hot clay/water suspension and stirred vigorously for 3 h at 80 ± 2 °C. The hot clay/water suspension was filtered, and the solid was washed several times with a tetrahydrofuran/warm water mixture (for 3 h) to remove free chloride ions. The washing was continued until the solid was verified for the absence of chloride ions by checking the aliquot filtrate solution with 0.1 N AgNO_3 solution.

The filtered clay was dried overnight at 70 °C. The modified clay was ground with a mortar and pestle and sieved to obtain particles with sizes less than 45 μm for the synthesis of vinyl ester nanocomposites. The nonreactive clay with 100 mol % undecyl amine hydrochloride (referred to as nonreactive C11 clay, NC11) was made by following a procedure similar to that described above.

Vinyl Ester Nanocomposites

First, either partially reactive or nonreactive C11 clay (0.3 g) was soaked in (1.5 g, 0.0144 mol) of

styrene, whereas Ashland Aotech Q6055 bisphenol A-type vinyl ester resin (5 g) was allowed to swell in styrene (1 g). After soaking the clay and resin in styrene for 3 h, both the clay and vinyl ester were combined and sonified with a Branson 2200 Ultrasonic Cleaner sonicator at 40-kHz frequency. The temperature was recorded and was 35 °C. Additional sonication experiments were performed with a high-power VWR Branson Ultrasonifier 250 R (frequency of 20 kHz) at a 40% duty cycle and at different output controls (from 1 to 10) for 30 min. During ultrasonication, the temperature of the mixture was maintained below 35 °C by placing the reaction vessel in an ice jacket. To the sonified mixture, *N,N*-dimethyl aniline (0.03 g, 0.00025 mol) and cobalt naphthenate (0.06 g) (catalyst) were added. The mixture was stirred for 5 min, after which methyl ethyl ketone peroxide (0.12 g, 0.00115 mol) was added. The mixture was then immediately poured into a dog-bone mold. The dog-bone specimen was precured for 30 min at 30 °C, postcured at 100 °C for 30 min, and cooled gradually in a Lab-Line Instrumentation programmable vacuum oven. The same curing cycle was used to prepare all vinyl ester nanocomposites, regardless of composition.

Thermogravimetric Analysis (TGA) of Nanoclay Powder

TGA was performed on the Na^+ clay, nonreactive C11 clay, and partially reactive C11 clay powder with a PerkinElmer 7 Series system in nitrogen atmosphere. The thermogram was generated by placing 25 mg of sample in a crucible and heating it from 30 to 600 °C at 20 °C/min. The nitrogen gas was allowed to flow at a rate of 5 mL/min. Similarly, TGA was also performed in air atmosphere to determine the mass of surfactant cations in the treated clays.

X-ray Diffraction (XRD) and Transmission Electron Microscopy (TEM) of Vinyl Ester Nanocomposites

The nanocomposite dog bone produced during the molding process had a fairly smooth surface. The dog-bone specimens with sample-to-sample variation in thickness were cut to size and analyzed by XRD with a Scintag, Inc. XRG 3000 diffractometer that was equipped with a Cu $K\alpha$ radiation source operated at 40 kV and 35 mA. The scanning speed and the step size were 0.01°/min and 0.04°, respectively.

TEM specimens were cut from dog bones with a Leica ultra-microtome, equipped with a diamond knife. They were collected on the surface of a water-filled trough and lifted from the surface with 200-mesh copper grids. Electron micrographs were taken with a Philips EM400T at an accelerating voltage of 120 kV.

RESULTS AND DISCUSSION

In this multistep synthetic strategy for forming the reactive surfactant, ω -undecylenol was initially converted to undecylenyl bromide. The purified undecylenyl bromide was characterized by FTIR and NMR techniques. The disappearance of the hydroxyl peak in the FTIR spectrum of ω -undecylenol [Fig. 2(a,b)] indicates the substitution of hydroxyl functionality with bromide. Further evidence for the conversion of ω -undecylenol to undecylenyl bromide is the absence of a primary alcohol proton peak at 2.44 δ in the ^1H NMR spectra of undecylenyl bromide (data are available but not provided). In comparison, the ^1H NMR spectra of ω -undecylenol (data are available but not provided) showed the primary alcoholic proton peak. Both of these ^1H NMR spectra showed the existence of vinylic proton peaks at approximately 5.8 ppm ($=\text{CH}-$) and 5.0 ppm ($\text{CH}_2=$), indicating the olefinic group at the terminal position of the sample, and hence the vinylic group was preserved during the conversion. The peak at ≈ 3.4 ppm was probably due to the α -methylene proton in the undecylenyl bromide compound.

In the second step, undecylenyl bromide was converted to undecylenyl azide. The azide was then reduced to an amine, followed by conversion to an amine hydrochloride [Fig. 2(c)]. Figure 3 shows the ^1H NMR spectrum of undecylenyl amine hydrochloride. The ^1H NMR spectrum had a peak at a chemical shift of 8.2 ppm, which was characteristic of the primary amine hydrochloride proton in the final compound. In addition, the ^1H NMR spectrum shows a α -methylene proton peak at 2.96 ppm, olefinic proton peaks at approximately 5.8 ppm ($=\text{CH}$), and at 4.93 ppm ($\text{CH}_2=$). The peaks at 4.93 and 5.8 ppm in the ^1H NMR spectrum clearly indicated that the vinyl group ($\text{CH}_2=\text{CH}$) was preserved during azide reduction and was available for further reaction.

The ^{13}C NMR spectrum for undecylenyl amine hydrochloride is depicted in Figure 4. The peak at 39.5 ppm can be assigned to the α -methylene

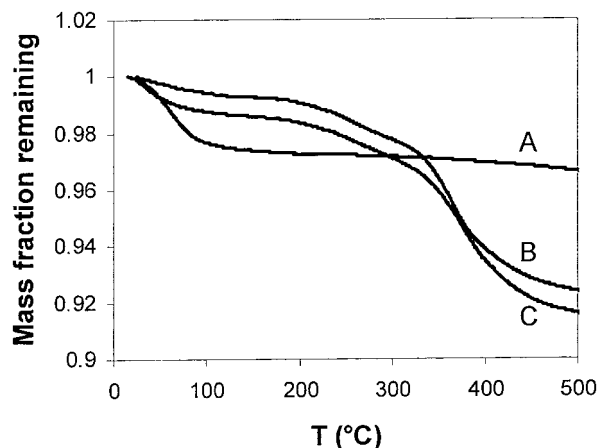


Figure 5. TGA of A, Na^+ clay; B, nonreactive C11 clay, NC11; and C, reactive C11 clay, RC11.

carbon. A vinylic methylene carbon peak appeared at 138.6 ppm and a vinylic methyne carbon peak appeared at 114 ppm. Other methylene carbon peaks appeared in the range of 25–33 ppm. As mentioned previously, the vinylic group was preserved during azide reduction and was available for reaction with the vinyl ester resin during the formulation of nanocomposite.

The CEC of Na^+ clay is reported to be 104 mmol/100 g.²¹ Figure 5 displays the TGA thermograms of Na^+ clay, nonreactive C11 clay, and partially reactive C11 clay. We assigned the low percentage mass loss at ≈ 100 °C to the loss of interparticle water. Thermal decomposition of the ammonium ions in the modified clay was most likely responsible for the drop in weight between ≈ 150 and 400 °C. This mass loss was absent in the Na clay. As a point of reference, pure octadecyl amine hydrochloride has a melting point of 155 °C and thermal decomposition of octadecyl ammonium salt from clay occurs at 210 °C (unpublished data). The onset decomposition temperature for ammonium salt, modified, organically layered silicate was shown to be 160 and higher.^{29,30} These observations supported our hypothesis that the thermal decomposition of undecyl amine salt should begin at ~ 150 °C. TGA was also performed in air atmosphere to measure the ammonium cation mass fraction in several different samples of treated clay: 87.5 ± 3.5 mmol/100 g of clay. This value agreed with the reported value.²¹

To confirm the observation that the Na^+ ions were replaced by undecyl ammonium ions, XRD of the organically modified clay and the Na^+ clay

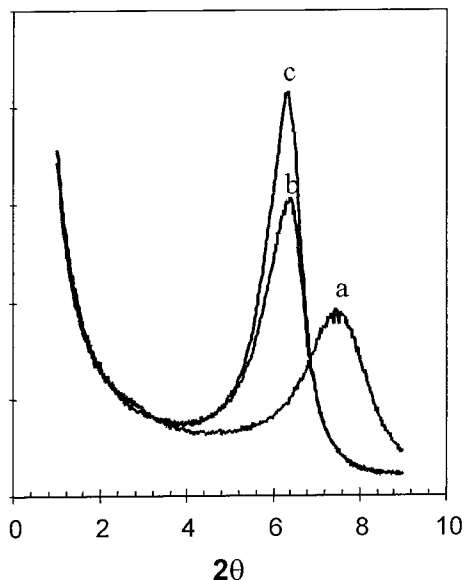


Figure 6. XRD of a, Na⁺ clay; b, NC11 clay; and c, RC11 clay.

was performed. The d -spacing of the undecyl amine hydrochloride modified clay was 1.40 ± 0.02 nm (for C11 treated nonreactive clay) and 1.39 ± 0.02 nm (for clay treated with a 25:75 mixture of reactive and nonreactive amine, respectively) as compared with 1.18 ± 0.02 nm for not fully dried Na⁺ clay (Fig. 6). These values were consistent with complete ion exchange by the organic cation. Specifically, these values indicated that the gallery spacing (t_{gallery}) after treatment was 0.42 and 0.41 nm, respectively [the thickness of the silicate layer (t_{silicate}) was 0.98 nm, as determined from fully dried MMT]. Assuming complete ion exchange (i.e., $f_{\text{cat}} = \text{CEC}$) and no residual water in the gallery, the density of the surfactant-filled gallery (ρ_{gallery}) relative to that of the silicate (ρ_{silicate}) is:

$$\frac{\rho_{\text{gallery}}}{\rho_{\text{silicate}}} = f_{\text{cat}} M_{\text{amine}} \frac{t_{\text{silicate}}}{t_{\text{gallery}}} \quad (1)$$

which, in this case, is 0.43. Here, M_{amine} is the molar mass of the ammonium ion. Because the density of the silicate is 2.0 g/cm^3 , this corresponds to a reasonable value for the gallery density of 0.86 g/cm^3 . Thus, it is likely that complete ion exchange was achieved. Because the uncertainty in t_{gallery} was approximately 5% (see above), the uncertainty of f_{cat} is likewise. Having achieved essentially complete ion exchange and

the resulting increase in d -spacing, further expansion by vinyl ester resin is possible.

After addition and curing of the vinyl ester resin, another peak at $2\theta = 3^\circ$ corresponding to intercalated clay was observed (Fig. 7). A small amount of resin lies within the gallery of the treated clay. The position and relative intensity of this peak is sensitive to the conditions used to prepare the composite material. The peak arising from treated clay (at $2\theta = 6.3^\circ$), however, remained prominent and indicated that matrix resin intercalation is not complete.

Although the d -spacing for these two peaks exhibited a ratio of nearly (but not exactly) 2:1, we did not interpret the higher order peak as a second order of the first, mainly because of their relative intensities. If the higher angle peak was a second order, reasonable models for the local electron density predict that the intensity of the second order should be significantly less than the first order. However, the observed intensity of the higher angle peak was comparable to, and even greater than, that of the low-angle peak associated with intercalated clay (giving rise to the peak at $2\theta = 3^\circ$). Therefore, a certain fraction of the clay was intercalated by polymer chain infiltration, and a certain fraction was nearly as-

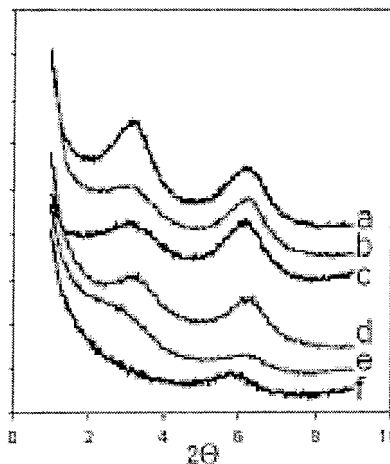


Figure 7. XRD of polymer clay composites. The peak at approximately 6.3° is associated with as-treated clay (see Fig. 6), and the peak at approximately 3° is associated with clay that is intercalated with resin. a, NC11, no styrene, low power; b, NC11, no styrene, high power; c, NC11, styrene, high power (the peaks are less intense); d, RC11, no styrene, low power; e, RC11, styrene, low power; less-intense diffraction; and f, RC11, styrene, high power; peak associated with intercalated structure is absent.

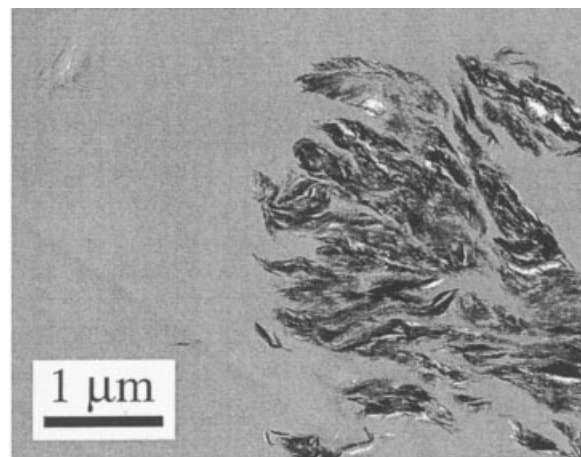
treated clay, that is, without polymer chain infiltration (peak at $2\theta = 6.3^\circ$).

Although efforts have been made in understanding the kinetic and thermodynamic parameters that control clay-platelet separation, many issues associated with the processing conditions as it relates to control of morphology remain unresolved. In this study, we consider some (thermodynamic) parameters (ultrasonication and the use of a swelling agent) that may promote diffusion of resin into the clay interlayer. To assess the role of the terminal functional group in promoting an intercalated/exfoliated structure, the XRD patterns of partially reactive and nonreactive C11 clay nanocomposite were also compared.

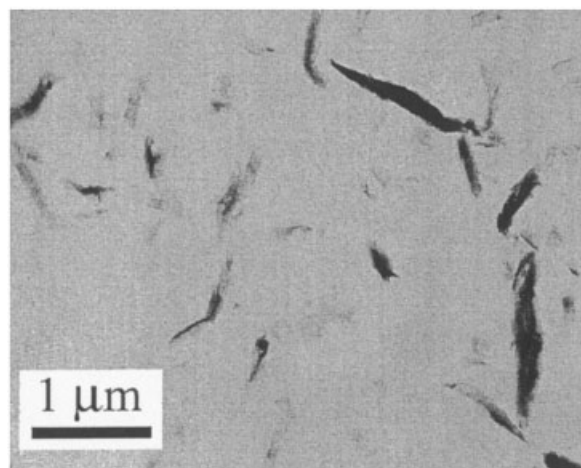
The relative amounts of exfoliated, intercalated, and as-treated clay and the size of the clay particle aggregates depended significantly on composition and processing, according to XRD and TEM analysis. It also appeared that the presence or absence of reactive amines influences the morphology. Weak hand mixing produced a poor dispersion, and the composite material was turbid. TEM micrographs revealed large, 1–10 μm aggregates [see Fig. 8(a)], the evidence of poor dispersion. A very small fraction of isolated, exfoliated silicate sheets are also observed. The great majority of silicate layers lie within the aggregates, and XRD reflections arising from intercalated and as-treated clay are observed (Fig. 7). Low-power sonication and heating before polymerization did little to change the morphology; both XRD peaks remained essentially unchanged with only slight sample-to-sample variations in the peak positions ($\pm 0.2^\circ$) and relative intensity.

The addition of a comonomer styrene and high-intensity ultrasonic mixing favor intercalation and exfoliation. Because mass transport of highly viscous resin into clay galleries is widely consid-

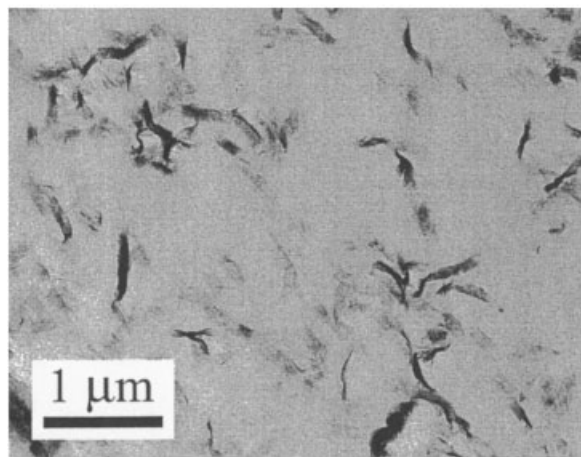
ered one of the limiting steps to exfoliation, the use of low-viscosity diluent and ultrasonication may indeed facilitate resin transport. Styrene



(a)



(b)



(c)

Figure 8. TEM micrographs of composite morphology: (a) NC11, no styrene, low power; large aggregates are scattered throughout the sample, and only a few individual (exfoliated) silicate plates are observed [cf. Fig. 7(a)]; (b) NC11, styrene, high power [small aggregates are well dispersed, and the exfoliated fraction is higher; cf. Fig. 7(c)]; and (c) RC11, styrene, high power [cf. Fig. 7(f)]. Images (b) and (c) are similar because aggregates of intercalated and as-treated clay are similar. The average aggregate size is slightly smaller in (c), and the degree of exfoliation is greater. Most exfoliated silicate particles are not observed edge on, so they appear as ribbons in these thin sections.

was chosen as the swelling agent and reactive diluent because it is widely used in vinyl ester preparation. The clay and vinyl ester were premixed with styrene to obtain a low-viscosity suspension in which efficient mixing of the various components can be achieved. Although styrene alone did not significantly change the *d*-spacing of the intercalated structure, the intensity of the intercalated clay peaks was reduced (Fig. 7). Some reduction was expected simply because of the lower concentration of silicate in the sample;³¹ an increased fraction of exfoliation caused further reduction in diffraction intensity at 3 and 6.3°. TEM micrographs of the composite showed many more small particles (aggregates) and some individual plates. Large aggregates persisted and the composite remained turbid.

Much higher power sonication breaks these large aggregates and produces a more uniform dispersion of small aggregates (typically several layers in thickness) and exfoliated particles [Fig. 8(b)], and the composite is comparatively more transparent. It is also reported³² that in polystyrene nanocomposite, sonication improves dispersion of clay platelets. The high-power ultrasonifer generates ultrasonic waves of high amplitude that induce cavitation bubbles as small as 10 μm. It is conceivable that these highly energetic bubbles when they form in the gallery spaces can induce deagglomeration of clay platelets. It is commonly reported in the literature^{18,33} that when the clay platelets are sufficiently separated and mixed with resin, often the viscosity of the system increases at low shear rates. In our study, we noticed an increase in the viscosity during and at the end of ultrasonication. This increase in viscosity happened because as the dispersion improved, the effective volume of clay platelets dramatically increased (consistent with the TEM images, Fig. 8).

Finally, treatment of the clay with the reactive amine produced the highest degree of exfoliation. When the high-power sonication was not used, and/or in the absence of styrene comonomer, both as-treated and intercalated XRD peaks were observed (Fig. 7), as before. These results were consistent with the TEM images of low-power sonicated RC11 clay polymer nanocomposites with no styrene and with styrene (data not shown). However, when high-power sonication was used to mix samples with styrene comonomer, the intercalated fraction decreased, and the composite was more transparent. Nevertheless, a fraction of as-treated clay remained in these composites; aggre-

gates were small (several silicate layers) and dispersed uniformly [Fig. 8(c)]. Most exfoliated silicate particles were not observed edge on; thus, they appeared as ribbons in these thin sections. Reaction of as-treated clay was not likely because of steric constraints, and the as-treated clay remained aggregated. Within the slightly expanded gallery of the intercalated clay, copolymerization of either vinyl ester or styrene with vinyl amine surfactant was possible, and the reaction could further promote exfoliation of these silicate layers.

Explanation of Formation of Exfoliated Nanocomposite

In clay-filled vinyl ester resin, the layer separation and polymer-network formation steps control the final morphology of nanocomposite. For formulating exfoliated nanocomposite, either the network structure of resin has to occur concurrently as the clay layer separates or layer separation should precede the network structure formation. For layer separation to occur while the network structure is being formed, the rate of layer separation must be considerably faster than the kinetics of the bulk network structure formation. To enhance the rate of gallery separation, generally the chemistry of organic modifiers on the exchanged clay surface is made compatible to the resin being investigated. The fundamental assumption is that organic modifiers can participate in the reaction(s) with resin components and improve the miscibility of the clay with resin. Specific associations between the functionalized clay and epoxy resin have been proposed in the formulation of epoxy nanocomposite.¹⁸ For example, it is assumed that the olefinic group in the undecenyl amine functionalized clay can react with styrene and/or vinyl ester resin, and/or a combination thereof. The intragallery reaction rate and the structural composition of network resin between the layers may well depend on the reactivity of the local components in clay layer spacing. One can envision the formation of copolymer structures, homopolymers, and the hybrid (clay/polymer interface) structure within the gallery.^{16,17} The characterization of vinyl ester nanocomposite to establish the coupling of surfactant-treated clay, comonomer, and/or matrix resin is a difficult and complex issue. In an attempt to address the chemical bonding aspect of chemically functionalized clay/vinyl ester nanocomposite, we performed a model experiment to study the reac-

tivity of reactive salt with styrene. Preliminary NMR data indicated (by loss of the alkenyl-proton signal) that the reactive salt copolymerizes with styrene monomer or homopolymerizes itself (work in progress). Indirect evidence for the bonding between reactive clay and resin can also be obtained by observing an increase in the viscosity of the clay/resin mixture and improvement in the stiffness and strength of nanocomposite. In our forthcoming article, we describe the mechanical property enhancement of reactive clay (hydroxyl and olefinic functional C19 amine hydrochloride surfactant-treated MMT clay) vinyl ester nanocomposite over nonreactive C18 clay vinyl ester nanocomposite and pristine resin.³⁴

In addition to the role of the partially reactive clay toward resin, there are kinetic and thermodynamic parameters that have to be considered in promoting exfoliation of clay platelets in vinyl ester resin. The addition of low-viscosity reactive monomer (styrene) generally facilitates the transport of higher viscosity resin in the gallery spacing and improves the swelling of the clay platelets because of nonpolar–nonpolar interactions (between the olefinic group in undecenyl amine-functionalized clay and the olefinic group in styrene). The transport of resin and comonomer in the gallery spacing of clay can be further facilitated by the use of an effective mixing technique. High-power sonication can effectively induce deagglomeration of clay platelets in the presence of low-viscosity reactive diluent.

We observed that it is the combination of partially reactive clay and mixing conditions that promotes layer separation and achieves a greater degree of exfoliation. Further studies have to be conducted to carefully evaluate the role of individual parameters in achieving morphological changes.

CONCLUSIONS

The following conclusions can be drawn from this work.

First, on the basis of characterization by ¹H NMR, ¹³C NMR, and FTIR techniques, the synthesis of reactive surfactant ω -undecylenyl (C11 with terminal vinyl) amine hydrochloride (from ω -undecylenol by a series of reactions that include bromination, azide formation, and azide reduction) was confirmed.

Second, by comparing the XRD and TGA results of the organically modified clay and the Na⁺

clay, we have shown that the Na⁺ ions have indeed been replaced by undecyl ammonium ions and/or undecenyl ammonium ions.

Third, an improvement in clay-platelet separation was achieved by making the clay sheets compatible with the vinyl ester resin and the selection of appropriate processing conditions. The addition of a comonomer styrene and high-intensity ultrasonic mixing favor intercalated and exfoliated clay-platelet morphology. Finally, treatment of the clay with the reactive amine produces the highest degree of exfoliation.

This work was supported by the Air Force Office of Scientific Research under grant F49620-01-1-0299. The authors acknowledge the involvement of G. Holmes from NIST in some useful discussions about the research. The authors thank M. Williams from NIST for assisting with the XRD measurements.

REFERENCES AND NOTES

- Vaia, R. A.; Giannelis, E. P. *MRS Bull* 2001, 26(5), 394–401.
- Calvert, P. *Nature* 1999, 399, 210–211.
- Gilman, J. W.; Jackson, C. L.; Morgan, A. B.; Harris, R., Jr. *Chem Mater* 2000, 12, 1866–1873.
- Kojima, Y.; Usuki, A.; Kawasumi, M.; Okada, A.; Fukushima, Y.; Kurauchi, T.; Kamigaito, O. *J Mater Res* 1993, 8, 1185–1189.
- Messersmith, P. B.; Giannelis, E. P. *J Polym Sci Part A: Polym Chem* 1995, 33, 1047–1057.
- Vaia, R. A.; Price, G.; Ruth, P. N.; Nguyen, H. T.; Lichtenhan, J. *Appl Clay Sci* 1999, 15, 67–92.
- Lagaly, G. *Appl Clay Sci* 1999, 15, 1–9.
- Yano, K.; Usuki, A.; Okada, A.; Kurauchi, T.; Kamigaito, O. *J Polym Sci Part A: Polym Chem* 1993, 31, 2493–2498.
- Qiao, F.; Li, Q.; Qi, Z.; Wang, F. *Polym Commun* 1997, 10, 135.
- Giannelis, E. P.; Bergman, J. S.; Chen, H.; Thomas, M. G.; Coates, G. W. *Chem Commun* 1999, 21, 2179–2180.
- Pinnavaia, T. J.; Wang, Z. *Chem Mater* 1998, 10, 3769–3771.
- Tolle, T. B.; Anderson, D. P. *Compos Sci Technol* 2002, 62, 1033–1041.
- Zilg, C.; Thomann, R.; Finter, J.; Mulhaupt, R. *Macromol Mater Eng* 2000, 280(1), 41–46.
- Akelah, A.; Kelly, P.; Qutubuddin, S.; Moet, A. *Clay Miner* 1994, 29, 169–178.
- Chin, I.; Thurn-Albrecht, T.; Kim, H.; Russell, T.; Wang, J. *Polymer* 2001, 42, 5947–5952.
- Kornmann, X.; Lindberg, H.; Berglund, L. *Polymer* 2001, 42, 4493–4499.
- Kornmann, X.; Berglund, L.; Sterte, J. *Polym Eng Sci* 1998, 38, 1351–1358.

18. Brown, J. M.; Curliss, D.; Vaia, R. A. *Chem Mater* 2000, 12, 3376–3384.
19. Butzloff, P.; D'Souza, N. A.; Golden, T. D.; Garrett, D. *Polym Eng Sci* 2001, 41, 1794–1802.
20. Ishida, H.; Campbell, S.; Blackwell, J. *Chem Mater* 2000, 12, 1260–1267.
21. Southern Clay Products, Literature.
22. Zerda, A. S.; Lesser, A. J. *J Polym Sci Part B: Polym Phys* 2001, 39, 1137–1146.
23. Barber, G. D.; Storey, R. F.; Moore, R. B. *Polym Prepr (Am Chem Soc Div Polym Chem)* 1999, 40, 768–769.
24. Wang, D.; Zhu, J.; Yao, Q.; Wilkie, C. A. *Chem Mater* 2002, 14, 3837–3843.
25. Koziara, A. *J Chem Res* 1989, S(9), 296–297.
26. Fabiano, E.; Golding, B. T.; Sadeghi, M. M. *Synth Stuttgart* 1987, 2, 190–192.
27. Koziara, A.; Osowska-Pacewicka, K.; Zawadzki, S.; Zwierzak, A. *Synth Stuttgart* 1985, 1, 202–204.
28. Certain commercial materials and equipment are identified in this article to adequately specify the experimental procedure. In no case does such identification imply the recommendation or endorsement by NIST, nor does it imply that these are necessarily the best available for the purpose.
29. Xie, W.; Gao, Z.; Pan, W. P.; Hunter, D.; Singh, A.; Vaia, R. *Chem Mater* 2001, 13, 2979–2990.
30. Davis, R. D.; Gilman, J. W.; Sutto, T. E.; Callahan, J. H.; Trulove, P. C.; Delong, H. C. *Appl Clay Sci*, in press, Nov. 11, 2003.
31. The mass fraction of treated clay in nanocomposite without styrene is approximately 5% and nanocomposite with styrene is approximately 4%.
32. Bourbigot, S.; Gilman, J. W.; VanderHart, D. L.; Awad, W. H.; Davis, R. D.; Morgan, A. B.; Wilkie, C. A. *J Polym Sci Part B: Polym Phys*, 2003, 31, 3188–3213.
33. Krishnamoorti, R.; Ren, J. X.; Silva, A. S. *J Chem Phys* 2001, 114, 4968–4973.
34. Balakrishnan, S.; Raghavan, D. *J Reinf Plast Compos*, accepted, 2003.